

# Crystallization and preliminary X-ray diffraction studies of *Escherichia coli* branching enzyme

Marta C. Abad,<sup>a</sup> Kim Binderup,<sup>b</sup>  
Jack Preiss<sup>b</sup> and James H.  
Geiger<sup>a\*</sup>

<sup>a</sup>Department of Chemistry, Michigan State University, East Lansing, MI 48824, USA, and

<sup>b</sup>Department of Biochemistry and Molecular Biology, Michigan State University, East Lansing, MI 48824, USA

Correspondence e-mail: geiger@cem.msu.edu

Branching enzyme catalyzes the formation of the branch points in glycogen and starch by cleavage of the  $\alpha$ -1,4 link and its subsequent transfer to the  $\alpha$ -1,6 position. This paper reports the crystallization and preliminary structural studies of an amino-terminally truncated branching enzyme from *Escherichia coli*. High-resolution diffracting crystals were obtained and a complete native data set to a resolution of 2.3 Å was collected. These crystals belong to the  $P2_1$  space group, with unit-cell parameters  $a = 91.44$ ,  $b = 102.58$ ,  $c = 185.41$  Å,  $\beta = 91.38^\circ$ . A native data set with 99.6% completeness, an overall  $R_{\text{merge}}$  of 0.086 and  $I/\sigma(I)$  of 10.43 was obtained.

Received 13 September 2001

Accepted 3 December 2001

## 1. Introduction

Branching enzyme (1,4- $\alpha$ -glucan:1,4- $\alpha$ -glucan 6-glucosyltransferase; EC 2.4.1.18) has an important role in the determination of the structure of starch in plants and of glycogen in animals and bacteria. This enzyme catalyzes the formation of the  $\alpha$ -1,6 branch points, transforming a linear polysaccharide into a branched network. This is achieved by cleavage of the  $\alpha$ -1,4-glucosidic linkage, yielding a non-reducing end polysaccharide chain, and subsequent attachment to the  $\alpha$ -1,6 position. This glycogen branching increases the number of non-reducing ends, thus making glycogen more reactive to synthesis and digestion, and is also essential for assuring its solubility in the cell. Accumulation of insoluble glycogen in the cell is known as glycogen-storage disease type IV (GSD IV) and is caused by mutations in the gene of the ubiquitously expressed glycogen-branching enzyme (Chen & Burchell, 1995; DiMauro & Tsujino, 1994). These mutations result in an impaired glycogen metabolism that forbids the formation of the branch points in glycogen, producing an insoluble polymer. GSD IV in its different forms affects the liver, muscular tissue and/or the central and peripheral nervous system.

Branching enzyme belongs to the  $\alpha$ -amylase family of enzymes (Baba *et al.*, 1991; Romeo *et al.*, 1988). Members of this group have the common function of cleaving and/or transferring glucose chains. This family has a common ( $\alpha/\beta$ ) barrel domain that contains the catalytic center of the enzyme (Jespersen *et al.*, 1991; Svensson, 1994). This catalytic center is composed of seven residues (Asp335, His340, Arg403, Asp405, Glu458, His525 and Asp526; *E. coli* branching enzyme numbering) which are conserved among members of this family such as  $\alpha$ -amylases, cyclodextrin glucano-

transferases, debranching enzymes, glucosidases and branching enzymes from different species. In an attempt to understand the catalytic relevance of these conserved residues, studies have been performed on maize endosperm branching enzyme using amino-acid replacement, chemical modification and site-directed mutagenesis. These studies revealed that His340, His525, Arg403, Asp335, Glu458 and Asp526 are necessary for the activity of branching enzyme (Cao & Preiss, 1999; Funane *et al.*, 1998).

The unique feature of the action of branching enzyme lies in its specificity for the length of the glucan chain transferred. Glycogen branching enzyme from *E. coli* has a preference for transferring shorter chains of between 5 and 16 glucose units. On the other hand, starch branching enzyme from maize has a higher propensity for transferring glucose chains of 6–30 glucose units (Guan *et al.*, 1997). This specificity is consistent with a much denser structure of glycogen compared with starch, with glycogen having twice the amount of  $\alpha$ -1,4 links (10%) than starch. We have crystallized a truncated form of the *E. coli* glycogen branching enzyme (N113GBE). This form lacked the first 112 residues at the amino-terminus, retaining approximately 50% of its branching activity (Binderup *et al.*, 2000). This truncated glycogen branching enzyme has an altered branching pattern, with a higher affinity for longer chains of 12 glucose units or more (Binderup *et al.*, 2002).

Although glycogen synthesis has been a field of study since the 1940s and progress has been achieved in the determination of its mechanism, its chemistry is not fully understood. This is mainly because of the lack of structural models. There are no structures of any of the branching enzymes involved either

in glycogen or starch biosynthesis. The three-dimensional structure of branching enzyme will reveal valuable information that will aid in the understanding of this biosynthetic pathway.

## 2. Materials and methods

The recombinant native and SeMet-substituted N113GBE enzyme was over-expressed in *E. coli* and purified as described elsewhere (Binderup *et al.*, 2000; Guan *et al.*, 1997). Protein homogeneity was verified by SDS-PAGE and the enzyme activity was determined using three different assays (Guan & Preiss, 1993). The purified protein was buffer exchanged in 25 mM Na HEPES pH 7.5 and concentrated to  $\sim 5$  mg ml<sup>-1</sup>.

## 3. Results and discussion

### 3.1. Crystallization

A homogeneous and active protein was screened for crystallization using the hanging-drop vapour-diffusion method. The reservoir contained 650  $\mu$ l of the precipitant solution and the 4  $\mu$ l hanging drop consisted of a 1:1 protein (5 mg ml<sup>-1</sup>) to precipitant solution ratio. The search for initial crystallization conditions was performed through sparse-matrix sampling using different screens at 298 and 277 K (Cudney *et al.*, 1994; Jancarik & Kim, 1991). The crystals formed at 277 K from a solution containing 100 mM Na HEPES pH 7.20. The crystals first appear after two weeks and reach maximum dimensions of 0.3  $\times$  0.1  $\times$  0.1 mm in four weeks (Fig. 1).

### 3.2. Diffraction data collection

The crystals were transferred to a cryoprotectant solution containing 25% (v/v) MPD, 2% (w/v) polyethylene glycol 4000 and 100 mM Na HEPES pH 7.5. The crystals

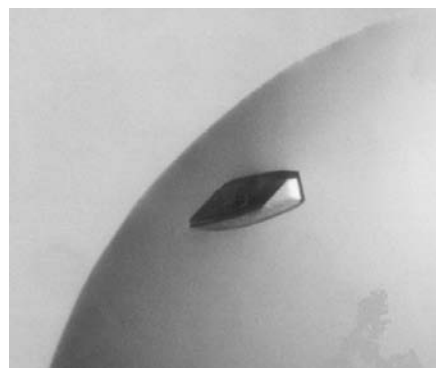


**Figure 1**  
A monoclinic crystal of glycogen branching enzyme. The crystals have dimensions of 0.3  $\times$  0.1  $\times$  0.1 mm.

**Table 1**

Statistics for the branching enzyme X-ray diffraction data collection.

Values in parentheses refer to the lowest resolution shell.

	Native†	SeMet‡	Hg soak§
Wavelength (Å)	0.97794	0.97938	1.54180
Resolution range (Å)	35.0–2.3 (2.38–2.30)	20–2.50 (2.59–2.50)	40–3.5 (3.63–3.50)
Unit-cell parameters (Å, °)	$a = 91.48, b = 102.56,$ $c = 185.10, \beta = 91.45$	$a = 91.65, b = 102.48,$ $c = 195.92, \beta = 91.68$	$a = 91.57, b = 102.79,$ $c = 185.58, \beta = 91.68$
Completeness (%)	99.6 (98.6)	94.2 (77.5)	91.5 (86.3)
$R_{\text{merge}} (I) \uparrow$ (%)	8.6 (30.3)	10.1 (29.2)	22.8 (50.0)
$\langle I \rangle / \langle \sigma(I) \rangle$ (%)	10.4 (2.6)	9.3 (1.5)	5.1 (2.34)

† Data collected at the Advanced Photon Source, Structural Biology Center ID19 beamline. ‡ Data collected at the Advanced Photon Source, IMCA beamline. § Data collected at Michigan State University Macromolecular X-ray Facility home source. ¶  $R_{\text{merge}} = \sum I_i - \langle I \rangle / \sum I_i$ , where  $I_i$  is an individual intensity measurement and  $\langle I \rangle$  is the average intensity for this reflection, with summation over all data.

were then mounted in nylon cryoloops (Hampton) and quickly frozen by immersion in liquid nitrogen. A high-resolution native data set was collected at the Advanced Photon Source (APS) at Argonne National Laboratories (Argonne, IL, USA) on the Structural Biology Center ID-19 beamline. Intensity data were collected using a 3  $\times$  3 array (3072  $\times$  3072 pixels) CCD area detector to a resolution of 2.3 Å. The crystal-to-detector distance was set to 220 mm and 160° of data were collected with an oscillation angle of 0.5°. Diffraction data were indexed and integrated using *DENZO* and scaled using *SCALEPACK* (Otwinowski & Minor, 1997).

The branching enzyme crystals belong to the  $P2_1$  space group, with unit-cell parameters  $a = 91.44, b = 102.58, c = 185.41$  Å,  $\beta = 91.38^\circ$ . Assuming four molecules of branching enzyme (71.6 kDa) per asymmetric unit, the crystal volume per protein mass is 3.1 Å<sup>3</sup> Da<sup>-1</sup>, which corresponds to approximately 56.5% solvent content in the crystal. This value is within the range observed for protein crystals (Matthews, 1968). Data were 99.6% complete for 152 002 unique reflections derived from a total of 499 161 reflections. Detailed data-collection statistics are given in Table 1.

SeMet-substituted protein was crystallized and cryoprotected under the same conditions as the native crystals and a single-wavelength anomalous dispersion (SAD) experiment was performed at the selenium absorption edge. Anomalous data to a resolution of 2.5 Å were collected in a single-element 165 mm MAR CCD detector at beamline 17-ID in the facilities of the Industrial Macromolecular Crystallography Association Collaborative Access Team (IMCA-CAT) at the Advanced Photon Source. The crystal-to-detector distance was set to 190 mm and 180° of data were collected (0.5° oscillation), with a total of 368 276 reflections measured (Table 1).

**Table 2**

Phasing power of the mercury-derivative and selenomethionine protein.

Phasing power,  $|F_H|/\sigma(\Delta)$ , determines the sharpness of the distribution function of the most probable phase, where  $\sigma(\Delta)$  refers to the r.m.s. lack of closure weighted by the phase probability and  $F_H$  is the structure-factor contribution of the derivative.

Resolution	Hg phasing power	Se phasing power, isomorphous	Se phasing power, anomalous
10.76	1.97	2.08	2.24
6.85	1.71	2.09	1.92
5.34	1.26	1.45	1.47
4.52	0.965	1.09	1.23
4.00	0.800	0.948	1.00
3.61	0.705	0.815	0.834
3.33		0.812	0.769
2.63		0.788	0.712

In addition to the SAD data, an isomorphous replacement experiment was performed. In this experiment, a native crystal was soaked for 18 h in a solution containing 10% MPD, 0.1 M Na HEPES pH 7.20 with 10  $\mu$ M of *p*-chloromercuribenzoic acid. The crystals were cryoprotected and frozen as previously detailed. Data was collected over 160° with oscillations of 1°. A total of 118 955 reflections were measured at our home source using a Rigaku R-AXIS IV<sup>++</sup> image-plate detector (Table 1). Cu  $K\alpha$  radiation was generated by a Rigaku RU-200 rotating-anode source operating at 50 kV and 90 mA. The structure will be determined using all three data sets for the identification of the selenium and mercury sites in branching enzyme by Patterson difference search routines followed by the calculation of an electron-density map. A table of the phasing power *versus* resolution for the mercury derivative and the selenium SAD data set is presented in Table 2.

This research has been supported in part by the Department of Energy grant DE-FGD2-93ER20121. Use of the Argonne National Laboratory Structural Biology

Center beamline at the Advanced Photon Source was supported by the US Department of Energy, Office of Biological and Environmental Research. The authors would like to thank Rongguang Zhang, Andrzej Joachimiak and Stephan L. Ginell from the Structural Biology Center at APS for their assistance throughout the data collection. We also thank Jorge Rios from the Industrial Macromolecular Crystallography Association for his contribution in the SAD data collection. These facilities are supported by the companies of the Industrial Macromolecular Crystallography Association through a contract with Illinois Institute of Technology (IIT), executed through the IIT's Center for Synchrotron Radiation Research and Instrumentation.

## References

- Baba, T., Kimura, K., Mizuno, K., Etoh, H., Ishida, Y., Shida, O. & Arai, Y. (1991). *Biochem. Biophys. Res. Commun.* **181**, 87–94.
- Binderup, K., Mikkelsen, R. & Preiss, J. (2000). *Arch. Biochem. Biophys.* **377**, 366–371.
- Binderup, K., Mikkelsen, R. & Preiss, J. (2002). In the press.
- Cao, H. & Preiss, J. (1999). *J. Protein Chem.* **18**, 379–386.
- Chen, Y. & Burchell, A. (1995). *Glycogen Storage Diseases*, Vol. 1, edited by C. Scriver, A. Beaudet, W. Sly & D. Valle, pp. 935–965. New York: McGraw-Hill.
- Cudney, R., Patel, S., Weisgraber, K., Newhouse, Y. & McPherson, A. (1994). *Acta Cryst.* **D50**, 414–423.
- DiMauro, S. & Tsujino, S. (1994). *Non-lysosomal Glycogenoses*, Vol. 2, edited by A. Engel & C. Franzini-Armstrong, pp. 1554–1576. New York: McGraw-Hill.
- Funane, K., Libessart, N., Stewart, D., Michishita, T. & Preiss, J. (1998). *J. Protein Chem.* **17**, 579–590.
- Guan, H., Li, P., Imparl-Radosevich, J., Preiss, J. & Keeling, P. (1997). *Arch. Biochem. Biophys.* **342**, 92–100.
- Guan, H. P. & Preiss, J. (1993). *Plant Phys.* **102**, 1269–1273.
- Jancarik, J. & Kim, S.-H. (1991). *J. Appl. Cryst.* **24**, 409–411.
- Jespersen, H. M., MacGregor, E. A., Sierks, M. R. & Svensson, B. (1991). *Biochem. J.* **280**, 51–55.
- Matthews, B. W. (1968). *J. Mol. Biol.* **33**, 491–497.
- Otwinowski, Z. & Minor, W. (1997). *Methods Enzymol.* **276**, 307–326.
- Romeo, T., Kumar, A. & Preiss, J. (1988). *Gene*, **70**, 363–376.
- Svensson, B. (1994). *Plant. Mol. Biol.* **25**, 141–157.